IEEE Access
Multidisciplinary | Rapid Review | Open Access Journal

Received March 1, 2021, accepted March 23, 2021, date of publication March 29, 2021, date of current version April 6, 2021.

Digital Object Identifier 10.1109/ACCESS.2021.3069409

Silver Sandwiched ITO Based Transparent Antenna Array for RF Energy Harvesting in 5G Mid-Range of Frequencies

NERMEEN A. ELTRESY[1], ABD ELHAMID M. ABD ELHAMID[2], DALIA M. ELSHEAKH[1,3], (Senior Member, IEEE), HADIA M. ELHENNAWY[4], AND ESMAT A. ABDALLAH[1], (Member, IEEE)

[1]Microstrip Department, Electronics Research Institute (ERI), El Nozha 12622, Egypt
[2]Nanotechnology Laboratory, Electronics Research Institute (ERI), El Nozha 12622, Egypt
[3]Electrical Department, Faculty of Engineering-Badr University, Badr University in Cairo, Badr 11829, Egypt
[4]Electronics and Communication Engineering Department, Ain Shams University, Cairo 11566, Egypt

Corresponding author: Nermeen A. Eltresy (nermeen@eri.sci.eg)

This work was supported by the National Telecommunication Regularity Authority (NTRA), Ministry of Communication and Information, Egypt.

ABSTRACT A transparent antenna array based on silver sandwiched indium tin oxide (AgITO) heterostructure thin films is presented. The AgITO is sputtered on both sides of soda-lime glass (SLG) substrate, and the three thin films deposition parameters are optimized to obtain very low ohmic interfacial contact resistance of less than 1 Ω/Sq. AgITO promotes thin film-based transparent microstrip structure of the proposed antenna array as well as the transparent T-junction power divider. Furthermore, AgITO microstrip as well as opaque single element antenna as reference antennas for a transparent array are presented. The proposed array has wide bandwidth promoting radio frequency energy harvesting at Wi-Fi 2.4, LTE 2600, WLAN, WiMAX and the expected 5G mid-bands. Moreover, it could be functionalized for wireless transmission within the previously mentioned bands. The transparent AgITO array has 5 dBi gain value against 2.3 dBi for the transparent AgITO single element antenna at 5.8 GHz. The array was utilized for radiofrequency energy harvesting, obtaining DC output volt=161.4 mV with a conversion efficiency of 32.9% at 5.8 GHz with RF received power of −10 dBm.

INDEX TERMS Harvesting, silver, ITO, transparent antenna array, transparent conductor, 5G.

I. INTRODUCTION

Radiofrequency energy harvesting (RF-EH) is drawing attention to power embedded sensors within internet of things (IoT). The IoT is applied for connecting physical devices with the internet using wireless sensors. Those sensors can be fixed or buried in hard-to-reach areas. The rapid growth of wireless devices leads to the existence of electromagnetic waves in closed areas along the day [1]–[4] Herein, RF-EH in conjunction with electrochemical storage device such as secondary batteries or supercapacitors is a promising candidate [5]–[7].

Among different types of antennas, the UV-transparent have potential applications in wireless communication on glass windows, cars without effecting eye vision. Modern applications such as IoT, and 5G transparent antennas (TAs) are essentially needed for decoration and security purposes. Besides, TAs are indispensable than opaque antennas in hybrid RF-solar harvesting. Various transparent single element antennas served for different applications were reported [8], [9]. However, low gain values were correlated with such designs due to relatively high sheet resistance (R_s) of the conductor patterns, high losses in the transparent conductor layer (TCL), and low conductor layer thickness [10]. Therefore, reducing losses within the TA conductor layer by dropping associated Rs while maintaining transparency is a real challenge.

The antenna's TCL usually obeys two main classifications, the first is meshed metal thin film patterns [11]–[13] while the other is transparent thin film patterns [14], [15]. There are many discrepancies between the meshed based designs and

The associate editor coordinating the review of this manuscript and approving it for publication was Zesong Fei.

conductive metal oxide films. The first promotes partial light transmission through the conductive layer itself whereas the metal lines block the light.

Despite using micromesh antenna for hybrid RF-Solar [16], transparent conductor oxides (TCOs) are more preferable to maximize the effective light-exposed area [8]. Transparent antenna array using mesh metal conductor layer is a good candidate for gain enhancement. A 60 GHz transparent patch 4 × 2 antenna array was fabricated using silver/titanium conductive mesh patterned on fused quartz substrate [11]. AgHT-4/AgHT-8 are commercially available silver-based meshes on a plastic substrate enabling fast access for the fabrication process of TA array [12], [13]. Unfortunately, mesh metal technology has drawbacks such as; low-frequency applications (4G/5G mid-range) that are hard to be achieved due to light trapping within the line cavities upon using high thickness and high meal thickness deposition limitation resulted from lattice strain/bandgap/thermal expansion coefficient mismatch between metal and the dielectric substrate.

There are commercially available thin films such as indium tin oxide (ITO) and fluorine doped tin oxide (FTO) with high transparency of 85-94%. However, these films have a high R_s around 8-10 Ω/Sq. Such relatively low conductivity causes two main drawbacks; (i) low antenna gain value and (ii) power distortion within the feeding network that blocks designing corresponding TA array. Furthermore, these commercially films coat only single side of transparent substrates which limited effective designing of different transparent antenna structures (only restricted in coplanar waveguide antennas). Many attempts were presented in [10], [15], [17]–[20] for improving the thin film conductivity, by adding metals like silver, gold or copper ultra-thin film with different low thickness ranging from 5 to 35 nm to the intrinsic TCL. Interestingly, the lowest achieved R_s due to metal/TCO is about 2.52 Ω/Sq, which still inconvenient for high-performance antenna application. In our previous work [21], the lowest reported R_s (0.9 Ω/Sq.) for a transparent thin film was obtained by deposition of silver sandwiched ITO (AgITO) heterostructure on a single side of glass substrate. As the developed AgITO film was applied for a TA, the gain is 3 dBi value against −2.9 dBi for transparent antenna based on commercially available ITO thin film.

In this paper, we boosted the using of AgITO coated two sides of glass substrate to promote the building of thin-film based microstrip structure transparent antennas (single element and array). The low R_s of AgITO enables 2 × 1 transparent antenna array with a transparent T-junction feeding network. Although the commercial glass is a non-ideal dielectric substrate compared to quartz or fused silica, it utilizes a real behavior for integrating such proposed antennas on smart buildings glassy sections. The designed antenna array has a wide operating frequency bandwidth that extends from 2.2 to 7.5 GHz for EH at Wi-Fi 2.4, LTE 2600, WLAN, WiMAX and the expected 5G mid-bands [22]. Fig. 1 illustrates images of the fabricated opaque reference single element antenna and

(a) (b)

FIGURE 1. Captured images of (a) Opaque reference single element antenna and (b) AgITO 2 × 1 transparent antenna array.

2 × 1 AgITO transparent antenna array on the Electronics Research Institute (ERI) logo. The paper is organized as the following: Section II represents designs of the single element antenna and the proposed AgITO transparent antenna array (AgITO TAA). In Section III, the fabrication and characterization process of AgITO TAA are illustrated. The results and discussions are presented in Section IV. Whereas RF-EH system measurement is detailed in section V. Lastly, Section VI concludes the work.

II. ANTENNA DESIGN

An opaque single element antenna was designed as a reference antenna using FR-4 substrate with 0.8 mm thickness, $\varepsilon_r = 4.5$ and $\tan\delta = 0.025$ coated with 0.035 mm thick copper as a conductor layer. An identical shape from our previously reported slot antenna in [21] is redesigned here and fed by 50 Ω microstrip feeding line. The opaque reference antenna design steps are presented in Fig. 2. Step (a) represents a monopole antenna and step (b) is a circular slot antenna. After that, the stub and the ground plane upper sides were grooved (step c and step d) to support different current paths to improve impedance matching at a wider operation band than conventional circular slot.

Fig. 3 (a) and (b) illustrate the impact of the antenna design steps on reflection coefficient and gain variation versus frequency, respectively. It can be seen that the final design (step d) has the highest gain value with nearly stable gain from 3 to 6 GHz. The same structure of the reference opaque antenna was applied using AgITO (transparent conductor layer with 227 nm thickness and sheet resistance Rs = 0.9 Ω/Sq.) coated two sides of soda-lime glass (SLG) substrate with $\varepsilon_r = 6$, $\tan\delta = 0.02$ and 1.1 mm thick. The antenna has a total area of 21.5 mm × 21.5 mm. Parametric study on the most important geometric parameters that affect our antenna to determine the maximum and minimum values for each parameter (range of each geometric parameter) was conducted after following the design steps. Finally, the genetic algorithm optimization in the Ansoft high-frequency structure simulator (HFSS) was used to optimize these parameters. Table 1 lists the single element antenna parameters.

A transparent antenna array was designed to increase the gain. The structure of the proposed AgITO TAA is illustrated in Fig. 4. The array was designed on SLG substrate coated

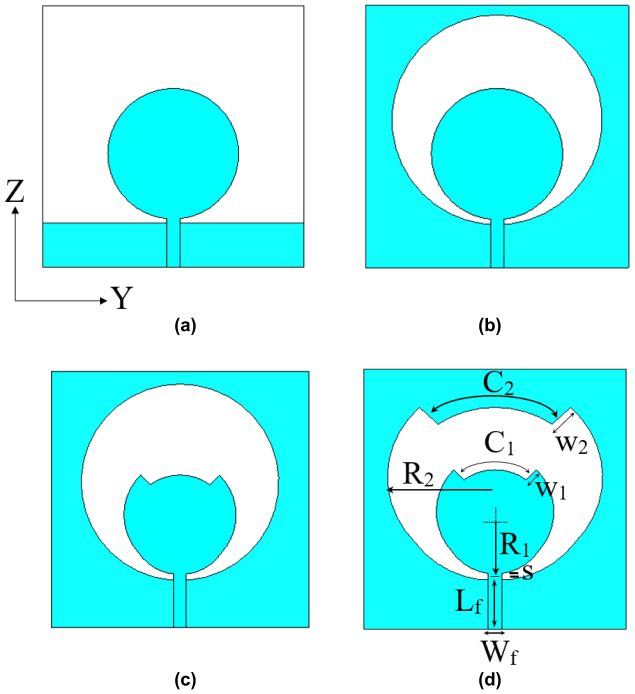

FIGURE 2. Design steps of the opaque reference single element antenna (a) First step, (b) Second step, (c) Third step and (d) Fourth step.

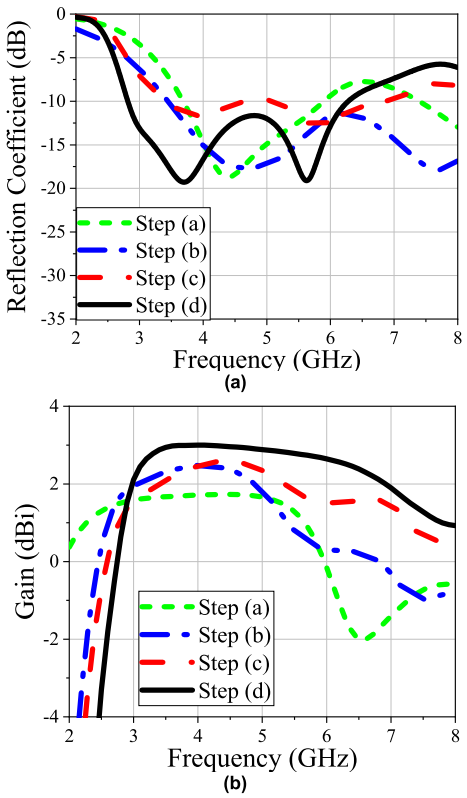

FIGURE 3. (a) Reflection coefficient, and (b) Gain variations versus frequency for design steps of the opaque reference single element antenna.

with AgITO. The array is fed using microstrip feeding line with impedance of $Z_o = 50\ \Omega$ which feeds T-junction

TABLE 1. Opimized geometric parameters of single element antenna.

Parameter	Value (mm)
w_f	1.5
L_f	4.2
S	0.4
R_1	4.3
w_1	1.2
c_1	5.5
R_2	9
w_2	2
c_2	10

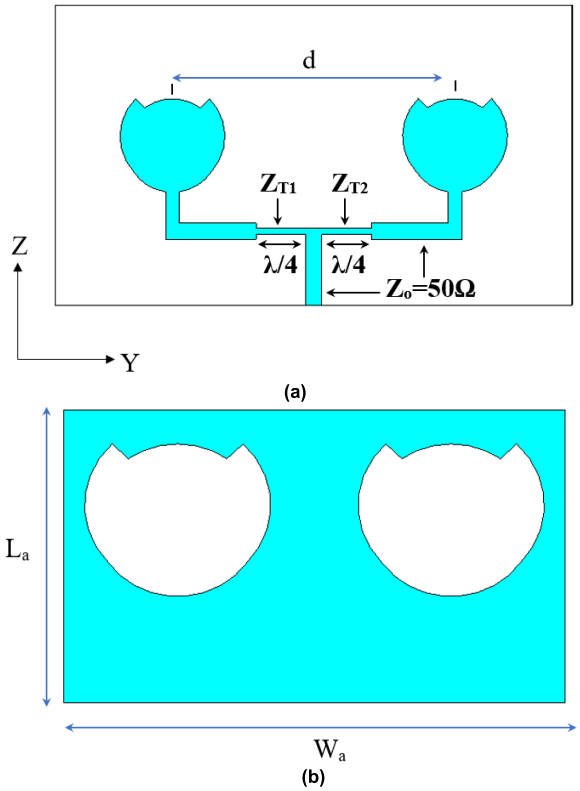

FIGURE 4. (a) Top, and (b) Bottom views of the 2 × 1 AgITO transparent antenna array.

power divider leading to the array elements, whereas the input impedance of the element is about 50 Ω. Consequently, λ/4 transformer with impedance of $Z_{T1} = Z_{T2} = 70.7\ \Omega$ is applied for efficient transmission between ($Z_1 = Z_2 = 100\ \Omega$) and $Z_o = 50\ \Omega$ of antenna elements, the widths of Z_o, ($Z_{T1} = Z_{T2}$) are 1.5, and 0.7 mm, respectively. The array has a total area of $W_a \times L_a = 4.76$ cm $\times 2.765$ cm and the separation distance between two radiating elements is d = 26 mm (λ/2 at 5.8 GHz) that is optimized to increase the gain performance of TA array. HFSS software was applied to design and simulate proposed antennas.

III. FABRICATION AND CHARACTERIZATION OF TA ARRAY

A. FABRICATION PROCESS OF AgITO TA ARRAY

The SLG substrates were cleaned by ethanol and acetone in ultrasound cleaner for 15min, respectively. Nitrogen gun was used to dry the samples of purity (99.99). The chamber was evacuated several times to a base pressure of 2×10^{-6} Torr via mechanical-turbo pump station then was backfilled with Ar (99.99) gas for purging. The typical procedure for AgITO array fabrication was described in our previous work [21]. Briefly, RF sputtering was used to deposit two ITO layers of 100 nm thickness. Whereas, the sandwiched Ag layer of thickness 27nm was deposited using DC sputtering. The 3 layers were deposited on pre-cleaned SLG substrate without breaking the vacuum except for coating the other glass side to maintain high quality and uniformity. ITO/Ag/ITO thin films thickness and deposition parameters were optimized to acquire the highest possible conductivity correlated with respectable transparency. Lastly, the double-sided coated glass was conducted to UV photolithography for associated pattern processing using a mixture of 1M HCl/HNO_3 (50:50) as a high rate etching agent. The opaque reference antenna is fabricated by UV photolithography using $FeCl_3$ etching agent.

B. CHARACTERIZATION OF AgITO THIN FILM, ANTENNAS, AND RF ENERGY HARVESTING SYSTEM

The AgITO thin film on SLG substrate was characterized using X'Pert pro (X-ray) and surface morphology was investigated using scanning electron microscope Quanta 250 FEG (SEM). The transparency was measured using LLG-uniSPEC 2 spectrophotometer. Four-prob technique (KEITHLEY Semiconductor Characterization System 4200-SCS equipped with four medium power source measurement units ''MP-4200-SMU) was used for AgITO sheet resistance measurements. The parameter analyzer Keithley 4200-SCS connected to Signatone probe station was used for AgITO sheet resistance measurement. The AgITO measurement is presented in Fig. 5, Rs = 0.91Ω/Sq. A schematic diagram and captured image of Van Der Pauw 4-probe setup are the inset figures. The SLG substrate dielectric constant and loss tangent were measured using the dielectric assessment kit System (DAKS-3.5 Speag).

The corresponding fabricated TA array reflection coefficient and the input impedance were measured using Rhode and Schwarz ZVA 67 vector network analyzer (VNA). Also, anechoic chamber (Star Lab.-007-A-0019) was used for radiation pattern measurements. RF generator (Anritsu-MG3697C), horn antenna, Tektronix MD04104C oscilloscope were functionalized for RF-EH measurement.

IV. RESULTS AND DISCUSSION

For the study of hybrid AgITO as a TCL, it was conducted to microscopic analysis as presented in Fig. 6 (a). The XRD spectrum showed a peak centered at 31.23° corresponding to

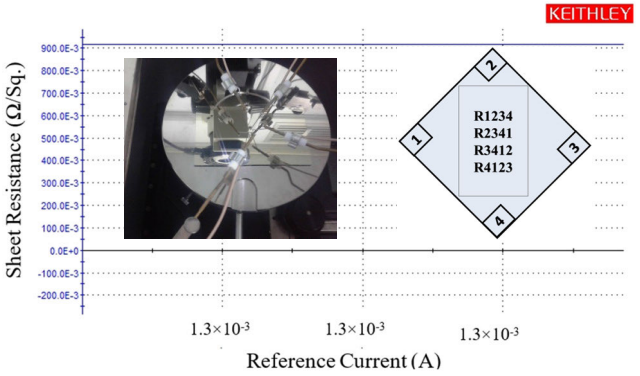

FIGURE 5. Measurement set up of AgITO sheet resistance.

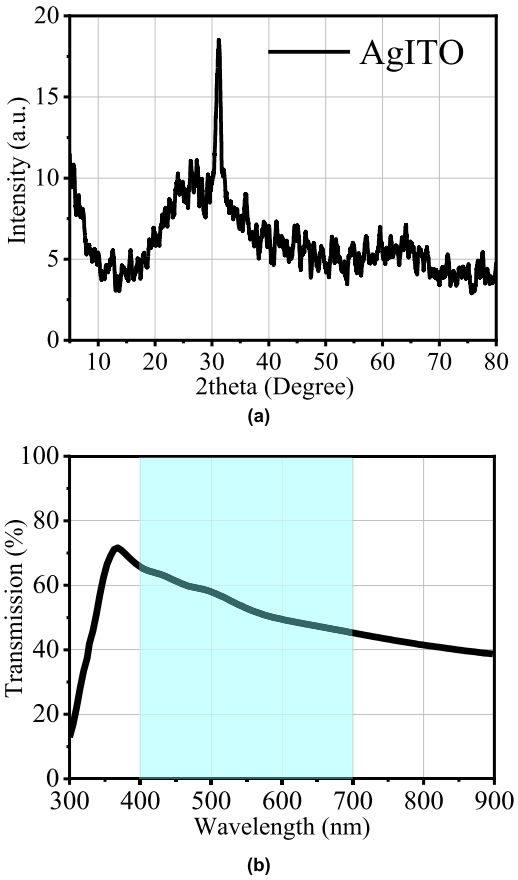

FIGURE 6. (a) XRD of AgITO thin films on SLG, (b) UV-Vis. Transparency spectrum.

ITO (222) facet (JCPDS card no. 06-0416) that is located on another broad hump at ∼25° generated by amorphous SLG. The silver peaks are absent due to low thickness and crystallinity as a result of using relatively low deposition temperature, which was essential for minimizing metallic Ag/ semiconductor ITO interfacial stress. Fig. 6 (b) illustrates transparency of the hybrid AgITO thin films from 300 to 900nm. At 550nm, the AgITO is 52.5%. Despite the comparable low transparency of the hybrid thin films, antenna's associated sheet resistance thin films at such low

thickness couldn't be attainable via traditional pure metal oxide. Therefore, metal should be impeded and to the best of our knowledge, the proposed AgITO thin films possess the lowest reported sheet resistance [23]–[25].

The SEM images (Fig. 7) present a good surface without significant defects. The 50μ one is indicating high film quality and homogeneity. Upon increasing the magnification to the 2μ scale, wrinkles-like structure dominates the surface that could only be attributed to the silver metal associated growth mode. The three layers of AgITO deposition parameters were optimized to provide the lowest sheet resistance correlated with the highest transparency. Although silver vacuum work function of about 4.4 eV is slightly lower than 8% doping ITO 4.5 eV, deposition parameters and thickness could lead to a slight change around those values [26], [27]. As metal/n-type semiconductor contact, Fermi levels will generate an ohmic IV attitude and electrons transfer from metal to semiconductor is expected. Nevertheless, the resulted sheet resistance suggests a negligible mismatch between the silver and ITO on terms of bandgap, which will make the three-layer structure acts as only one compacted structure of a nearly perfect conductor with high carriers' mobility and concentration [28], [29].

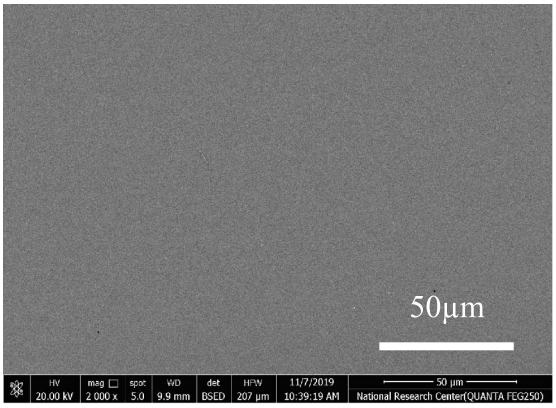

(a)

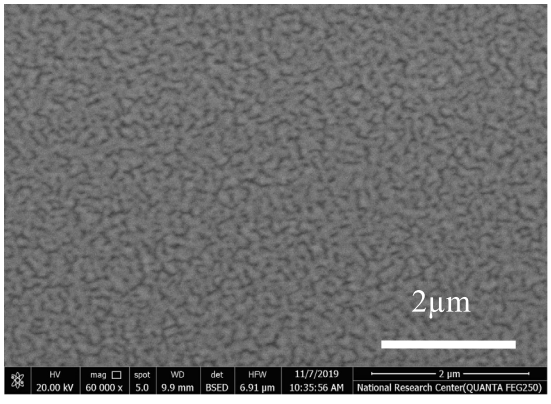

(b)

FIGURE 7. SEM images at different magnification scales of (a) 50μm and (b) 2μm.

The fabricated opaque and AgITO single element antennas reflection coefficients variation versus frequency were measured and compared with the simulated results. The results are illustrated in Fig. 8 where a good agreement between simulated and measured results for both antennas can be observed. Opaque and transparent single element antennas have a nearly operating bandwidth of 2.5-6.5 GHz. Despite losses in AgITO thin film, the results proved a metal -like-attitude with frequency. The performance of AgITO TAA was studied in terms of reflection coefficient, input impedance, gain, and radiation pattern. Fig. 9 (a) presents a good agreement between simulated and measured reflection coefficient variation with frequency for AgITO TAA. A wide BW of 2.2-7.5 GHz with fractional bandwidth (FBW) = 106% relative to F_o = 5 GHz and S11<−10dB is achieved. The array input impedance is 48-j13 Ω at 5.8 GHz as shown in Fig. 9 (b). A comparison between simulated current distributions of the proposed opaque array (reference) and transparent antenna array at 5.2 and 5.8 GHz are shown in Fig. 10. As hypothesized, current distribution of opaque reference antenna array is higher than AgITO TAA. Interestingly, the high current distribution on the feeding network of TAA indicates the low losses on its feeding network due to the low sheet resistance value.

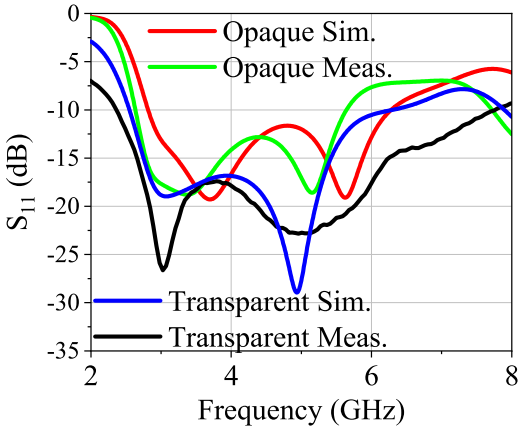

FIGURE 8. Reflection coefficient variation versus frequency for opaque and AgITO transparent single element antennas.

A comparison between the single element antennas (opaque, transparent) and the AgITO TAA according to their gain variation versus frequency is presented in Fig. 11. The peak gain of AgITO TAA is 5 dBi at 5.8 GHz against 2.7 dBi, 2.3 dBi for opaque and transparent single element antennas, respectively. The AgITO TAA has higher gain than the AgITO single element antenna through 4.5-7.3 GHz only (not all the operating band) because the AgITO TAA is fed using T-junction with λ/4 transformer which was designed corresponding to 5.8 GHz moreover that the distance between the two elements in the array was d=26 mm (λ/2 at 5.8 GHz). Generally, the AgITO TAA has more than 3 dBi gain value over frequency bandwidth of 4.6-6.8 GHz with stable behavior and provides positive gain value despite using lossy

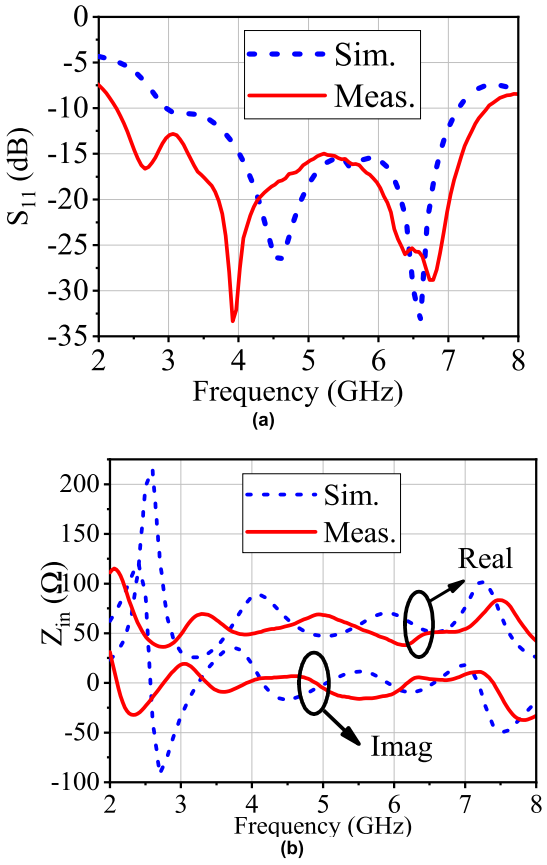

FIGURE 9. (a) Reflection coefficient, and (b) Input impedance variations versus frequency for the AgITO TAA.

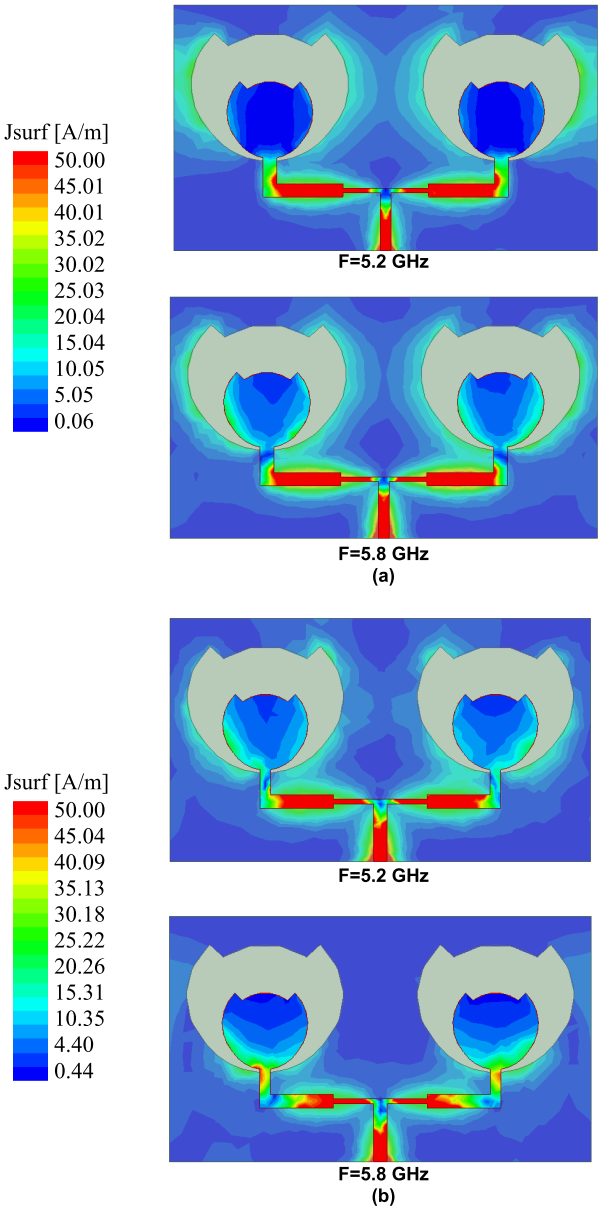

FIGURE 10. Current distribution at 5.2, and 5.8 GHz for (a) Opaque reference antenna array, and (b) Transparent AgITO TAA.

thin-film TCL over frequency bandwidth of 3-7.2 GHz. The relatively high AgITO based antennas performance is attributed to (i) relatively low sheet resistance of AgITO which is unattainable via commercially available single side coated transparent substrates, (ii) using slot antenna structure of wideband operation and stable parameters, and (iii) optimizing the array dimensions (distance between the two elements, feeding network).

The proposed antennas radiation efficiency variation versus frequency is shown in Fig. 12. It can be seen that the opaque single element antenna has higher efficiency than AgITO transparent single element antenna. The TAA has approximately 71% radiation efficiency at 5.2 and 5.8 GHz. A good agreement between simulated and measured AgITO TAA radiation pattern is illustrated in Table 2. A figure of eight in both H and E planes are presented indicating radiation in both directions (forwards and backwards), which is preferable in RF-EH application.

Table 3 presents a comparison between the current work and others' related reports. The table contains heterostructures thin films-based antennas performance below 6 GHz (currently available BW for RF-EH). A metal enhanced TCO is proved to increase surface conductivity against the crude structure. As the metal thickness increases, a systematic transparency drop is expected. At a certain thickness, the metal layer is transformed into opaque appearance which prevents a multilayer ohmic structure to be less than 1Ω/Sq. especially on using $\leq 1\mu$m TCL thickness. Using an opaque ground (GND) enhances the gain but vanishes the transparency advantage. Moreover, 2D designs are compatible with various applications such as RF-EH, IoT and smart houses rather than 3D type. Besides, noble metal deposition like gold on a metal oxide layer is not convenient in various applications due to very low metal film adhesion and Vollmer-Weber growth mode resulting 3D isolated islands at low metal thickness [30]. Nevertheless, the AgITO TCL presents a 2D, stable metal layer and low sheet resistance. As far as we know, this is the first silver enhanced TCO continuous thin film-based TA array.

Besides low Associated AgITO sheet resistance and high-performance electromagnetic performance [21]

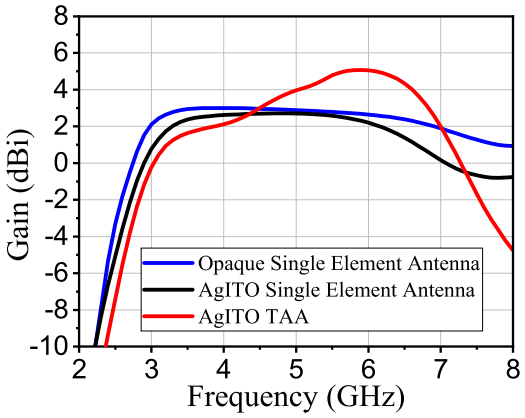

FIGURE 11. Gain variation versus frequency for single element antennas and AgITO TAA.

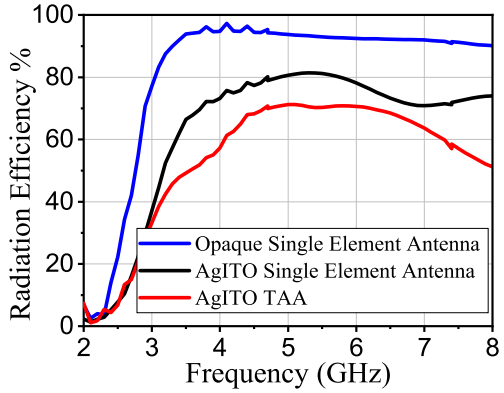

FIGURE 12. Radiation efficiency variation versus frequency for single element antennas and AgITO TAA.

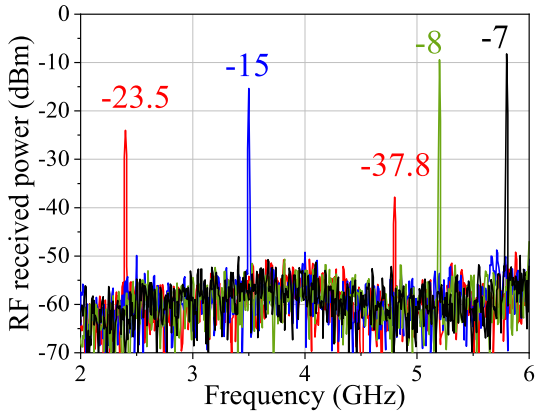

FIGURE 13. The RF received power by the AgITO TAA from horn antenna at distance of 20 cm.

thin-film based TAA possess many features over silver-coated polyester film AgHT like surface native oxide that protect structures from ageing and corrosion effects. There is no need for using cutting or gluing on another substrate forming inconvenient processing and multilayers complex dielectric constants, the alignment of the array in such case is a manual process that makes the process is not applicable in real

TABLE 2. Radiation pattern of AgITO TAA in E and H planes.

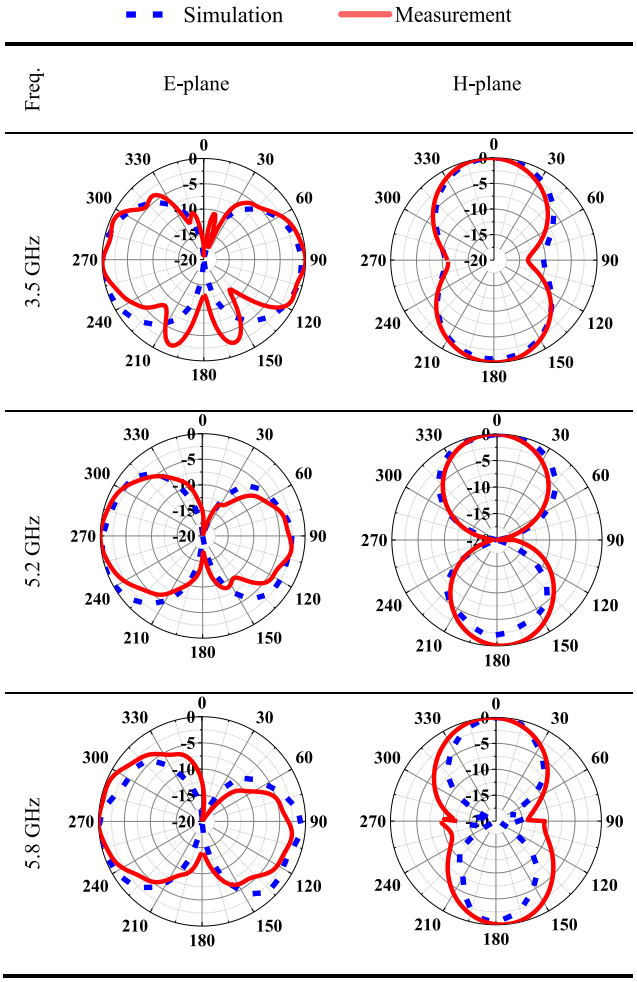

applications while AgITO uses traditional UV photolithography [13] [12]. Despite the relatively AgITO losses caused by skin depth and sheet resistance when compared to thick meshed metal arrays, there are many advantages such as; no need for expensive cleanroom processing, the complexes of upper versus lower patterns alignment that affect visual transparency as well as electromagnetic performance and shifts the antennas operating frequency [11], [32], [33]. The proposed AgITO TAA feeding network possess the exact transparency like the whole patterns contrary to the meshing type that uses a dense structure to provide low sheet resistance but low transparency as the current distribution is maximized. Applying non-ideal dielectric substrate to develop a real behavior for integrating such proposed antennas on smart buildings glassy sections.

There is a major discrepancy based on using different CPW and Microstrip structure. On the first hand, CPW antenna is based on single side coated conductive film of low gain with no possibility of making an array. On the other hand, the microstrip design is built of a double coating conductive film. Interestingly, there are no double-side transparent commercially available products including ITO/FTO/AgHT.

TABLE 3. Comparison of proposed TAs with other work.

Ref.	Film	Rs (Ω/Sq.)	T (%)	Peak Gain (dBi)@Freq. (GHz)	η_{rad} (%)	Structure/Antenna/GND/ Area (mm^2)
[10]	IZTO/Ag/IZTO	2.52	80	-4.23@2.5	7.76	2D/Transp. patch/Transp./50×50
[15]	ITO	10	-	-8@4	-	2D/Transp. monopole/Transp./50×50
	ITO/Cu	2.732	-	-1.2 @ 4	-	
[14]	ITO	8.6	69<T<86	-4.1@0.8	-	3D/Transp. monopole/Opaque/150×150
	ITO/Cu/ITO	4.7	28<T<61	-1.96@ 0.8	-	
[19]	ITO/Ag/ITO	5	37<T<74	4@ 3.5	-	3D/Transp. monopole/Opaque/300×300
[18]	ITO	15	88	-2@5	25	2D/Transp. monopole/Transp./49.5×50
	ITO/gold	5	55	2.2@5	67	
[20]	IZTO/Ag/IZTO	4.99	81.1	2.89@2.45	34.8	3D/Transp. monopole/opaque/24.8× 2
[21]	ITO	8	85-93.7	-2.9@ 5.8	21	2D/Transp. CPW slot/Transp./29×29
	ITO/Ag/ITO	0.9	66-45.3	3@ 5.8	73.2	2D/Transp. CPW slot/Transp./29×29
This	ITO/Ag/ITO	0.9	66-45.3	2.3 @ 5.8	80	2D/Transp. microstrip slot/Transp./29×29
work	ITO/Ag/ITO	0.9	66-45.3	5@ 5.8	70.8	2D/Transp. microstrip array/Transp./47.6×27.65

This work is an expansion of the published letter as we expand our understanding of this low resistance heterostructure AgITO electromagnetic behavior and study the array performance. Moreover, The T-junction is fabricated using transparent AgITO for the first time. The major problem of making double-coated structure is conducting one of the two sides to double treatments of substrate heating, back deposition and RF reactive ions during the other side deposition. Therefore, the multilayers and semiconductors-based thin films structure are highly affected and the conductivity will drop to tenths of ohms/cm^2. We overcome such drawbacks in our deposited double side AgITO heterostructure films by crucial variation of deposition parameters.

V. RF-EH SYSTEM

The AgITO TAA was tested by using a wideband horn antenna that has 10.2, 11.8 dBi gain values at 5.2, and 5.8 GHz, respectively as a transmitter antenna. The AgITO TAA to horn distance was fixed at 20 cm, where the RF received power was measured using the oscilloscope as a spectrum analyzer on RF mode. Fig. 13 illustrates the RF received power variation versus frequency by AgITO TAA using 10 dBm transmitted power.

The AgITO TAA was applied for RF-EH system in Fig. 14 (a) which consists of RF source (horn antenna), receiving antenna AgITO TAA, simple half-wave rectifier circuit (HWR) [34], matching circuit in between the AgITO antenna and the HWR. The matching circuit consists of short ended stub with 4.5 mm length and it is used to match the input impedance of the receiving antenna (around 50 Ω) with the input impedance of HWR circuit (≠50Ω). For obtaining the DC output volt, the SMS7630 Schottky diode is used in the HWR circuit [35]. The output volt is taken through a smoothing capacitor (C=1pf) and a parallel load resistor ($R_{L=}$ = 750 Ω). The rectifier circuit is designed to operate

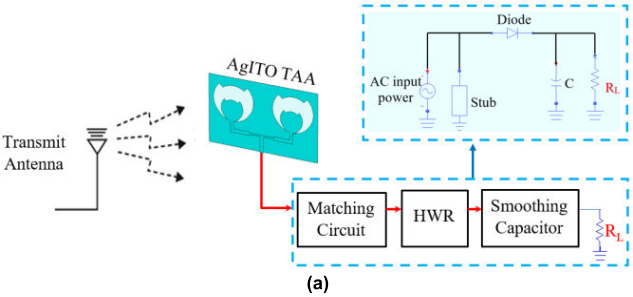

(a)

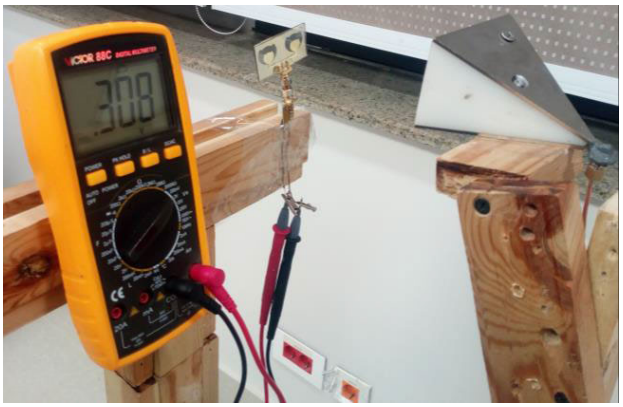

(b)

FIGURE 14. (a) RF-EH system diagram, and (b) Image of Vo on voltage meter.

at 4.5-6 GHz where maximum DC output volt and conversion efficiency are located. However, it can be conducted to work at the wideband AgITO TAA first frequency region at 2.4 and 3.5 GHz with lower output volt [8], [36].

For obtaining the output volt at different levels of received RF power (P_r), the horn is fed by RF generator with different levels of transmitted power (P_T = 0-30 dBm) at *5.2*,

and *5.8 GHz*. A voltmeter was used to monitor the DC output voltage (V_o) through the load resistance. Fig. 14 (b) shows the rectenna array V_o =0.308 volt for received power (P_r) = −5 dBm at 5.8 GHz. Fig. 15 (a) presents the array's V_o versus P_r for the four frequencies. Fig. 15 (b) shows the estimated rectenna efficiency versus P_r using the rectenna conversion efficiency equation [37]. The rectenna array attends a maximum efficiency of 46.8%, 53.5% at 5.2 and 5.8 GHz, respectively.

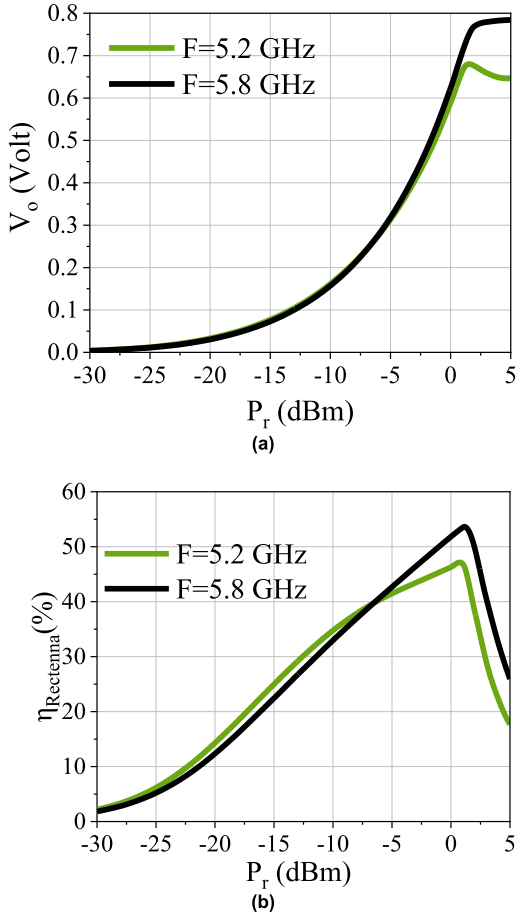

FIGURE 15. AgITO TAA (a) V_o, (b) Efficiency variation versus RF received power.

Despite the TAA expected low rectenna efficiency at the lower band of frequencies, it's a common case in multiband RF-EH where rectenna efficiency is not high for all the different operating frequency bands. A low efficiency could be obtained due to the lower value of the antenna efficiency at the corresponding frequency and also due to poor impedance matching between the antenna and rectifier at the concerned frequency compared to single-band RF-EH [39]. In a real harvesting case, the ambient RF power is not stable and available all day at one specific frequency according to the conducted RF spectrum study presented in [40]. In other words, no specific RF band provides the highest RF-EH capability. Therefore, multiband RF-EH system in conjunction with rechargeable batteries or supercapacitors is the most practical solution [40]–[42].

VI. CONCLUSION

Thin film-based transparent microstrip antennas (single element and antenna array) have been presented. The sputtered AgITO conductive thin film on double-sided SLG deposition parameters were optimized to promote the lowest reported thin-film sheet resistance of about 0.9 Ω/Sq., the applied microscopic analysis on the AgITO thin-film proved high quality and homogeneity. AgITO transparent single element antenna and the AgITO transparent antenna array were designed and fabricated by patterning the double side coated SLG substrate. The AgITO TAA achieves reasonable gain (< 3 dBi) over frequency wide bandwidth of 4.6-6.8 GHz with a maximum gain of 5 dBi and 70.8% radiation efficiency at 5.8 GHz. The AgITO TAA has a stable forward and backward radiation pattern over a wide bandwidth. Finally, the harvested volt at −5 dBm received power was about 0.308V that could enable successful integration with EH system' applications on glass windows.

REFERENCES

[1] B. Alzahrani and W. Ejaz, "Resource management for cognitive IoT systems with RF energy harvesting in smart cities," *IEEE Access*, vol. 6, pp. 62717–62727, 2018.
[2] W. Ejaz, M. Naeem, M. Basharat, A. Anpalagan, and S. Kandeepan, "Efficient wireless power transfer in software-defined wireless sensor networks," *IEEE Sensors J.*, vol. 16, no. 20, pp. 7409–7420, Oct. 2016.
[3] A. Takacs, A. Okba, H. Aubert, S. Charlot, and P.-F. Calmon, "Recent advances in electromagnetic energy harvesting and wireless power transfer for IoT and SHM applications," in *Proc. IEEE Int. Workshop Electron., Control, Meas., Signals Appl. Mechatronics (ECMSM)*, May 2017.
[4] K. Shafique, B. A. Khawaja, M. D. Khurram, S. M. Sibtain, Y. Siddiqui, M. Mustaqim, H. T. Chattha, and X. Yang, "Energy harvesting using a low-cost rectenna for Internet of Things (IoT) applications," *IEEE Access*, vol. 6, pp. 30932–30941, 2018.
[5] L. M. Borges, R. Chávez-Santiago, N. Barroca, F. J. Velez, and I. Balasingham, "Radio-frequency energy harvesting for wearable sensors," *Healthcare Technol. Lett.*, vol. 2, no. 1, pp. 22–27, 2015.
[6] A. D. Ball, F. Gu, R. Cattley, X. Wang, and X. Tang, "Energy harvesting technologies for achieving self-powered wireless sensor networks in machine condition monitoring: A review," *Sensors*, vol. 18, no. 12, pp. 1–39, 2018.
[7] H. H. Ibrahim, M. S. J. Singh, S. S. Al-Bawri, and M. T. Islam, "Synthesis, characterization and development of energy harvesting techniques incorporated with antennas: A review study," *Sensors*, vol. 20, no. 10, pp. 1–27, 2020.
[8] T. Peter, T. A. Rahman, S. W. Cheung, R. Nilavalan, H. F. Abutarboush, and A. Vilches, "A novel transparent UWB antenna for photovoltaic solar panel integration and RF energy harvesting," *IEEE Trans. Antennas Propag.*, vol. 62, no. 4, pp. 1844–1853, Apr. 2014.
[9] M. R. Haraty, M. Naser-Moghadasi, A. A. Lotfi-Neyestanak, and A. Nikfarjam, "Transparent flexible antenna for UWB applications," *Appl. Comput. Electromagn. Soc. J.*, vol. 31, no. 12, pp. 1426–1430, 2016.
[10] S. Hong, Y. Kim, and C. W. Jung, "Transparent microstrip patch antennas with multilayer and metal-mesh films," *IEEE Antennas Wireless Propag. Lett.*, vol. 16, pp. 772–775, 2017.
[11] A. Martin, O. Lafond, M. Himdi, and X. Castel, "Improvement of 60 GHz transparent patch antenna array performance through specific double-sided micrometric mesh metal technology," *IEEE Access*, vol. 7, pp. 2256–2262, 2019.
[12] J. L. Kubwimana, N. J. Kirsch, C. Ziegler, G. Kontopidis, and B. Tuner, "Dual-polarized 5.75 GHz optically transparent antenna arrays," *IEEE Antennas Wireless Propag. Lett.*, vol. 18, no. 7, pp. 1512–1516, Jul. 2019.

[13] A. Desai, T. Upadhyaya, M. Palandoken, and C. Gocen, "Dual band transparent antenna for wireless MIMO system applications," *Microw. Opt. Technol. Lett.*, vol. 61, no. 7, pp. 1845–1856, Jul. 2019.

[14] F. Colombel, E. M. Cruz, M. Himdi, G. Legeay, X. Castel, and S. Vigneron, "Ultrathin metal layer, ITO film and ITO/Cu/ITO multilayer towards transparent antenna," *IET Sci., Meas. Technol.*, vol. 3, no. 3, pp. 229–234, May 2009.

[15] L. Cai, "An on-glass optically transparent monopole antenna with ultra-wide bandwidth for solar energy harvesting," *Electronics*, vol. 8, no. 916, pp. 1–9, 2019.

[16] Y. Zhang, S. Shen, C. Y. Chiu, and R. Murch, "Hybrid RF-solar energy harvesting systems utilizing transparent multiport micromeshed antennas," *IEEE Trans. Microw. Theory Techn.*, vol. 67, no. 11, pp. 4534–4546, Nov. 2019.

[17] C. Guillén and J. Herrero, "ITO/metal/ITO multilayer structures based on Ag and Cu metal films for high-performance transparent electrodes," *Sol. Energy Mater. Sol. Cells*, vol. 92, no. 8, pp. 938–941, Aug. 2008.

[18] M. R. Haraty, M. Naser-Moghadasi, A. A. Lotfi-Neyestanak, and A. Nikfarjam, "Improving the efficiency of transparent antenna using gold nanolayer deposition," *IEEE Antennas Wireless Propag. Lett.*, vol. 15, pp. 4–7, 2016.

[19] J. Hautcoeur, F. Colombel, X. Castel, M. Himdi, and E. M. Cruz, "Radiofrequency performances of transparent ultra-wideband antennas," *Prog. Electromagn. Res. C*, vol. 22, pp. 259–271, Jul. 2011.

[20] S. Hong, S. H. Kang, Y. Kim, and C. W. Jung, "Transparent and flexible antenna for wearable glasses applications," *IEEE Trans. Antennas Propag.*, vol. 64, no. 7, pp. 2797–2804, Jul. 2016.

[21] N. A. Eltresy, A. M. A. Elhamid, D. N. Elsheakh, E. A. Abdallah, and H. M. Elhennawy, "AgITO for high-performance semi-transparent wideband antenna applications," *Electron. Lett.*, vol. 56, no. 15, pp. 749–750, Jul. 2020.

[22] C.-Y.-D. Sim, H.-Y. Liu, and C.-J. Huang, "Wideband MIMO antenna array design for future mobile devices operating in the 5G NR frequency bands n77/n78/n79 and LTE band 46," *IEEE Antennas Wireless Propag. Lett.*, vol. 19, no. 1, pp. 74–78, Jan. 2020.

[23] M. Sawada, M. Higuchi, S. Kondo, and H. Saka, "Characteristics of indium-tin-oxide/silver/indium-tin-oxide sandwich films and their application to simple-matrix liquid-crystal displays," *Jpn. J. Appl. Phys.*, vol. 40, no. 5A, pp. 3332–3336, May 2001.

[24] S. W. Chen, C. H. Koo, H. E. Huang, and C. H. Chen, "Ag–Ti alloy used in ITO–metal–ITO transparency conductive thin film with good durability against moisture," *Mater. Trans.*, vol. 46, no. 11, pp. 2536–2540, 2005.

[25] S. K. Jung and S. H. Sohn, "Electrical and optical properties of multilayered $(ITO/Ag/ITO)_n$ transparent conductive films grown onto PET substrates," *Mol. Crystals Liquid Crystals*, vol. 513, no. 1, pp. 301–310, Nov. 2009.

[26] F. Parmigiani, E. Kay, T. C. Huang, J. Perrin, M. Jurich, and A. J. D. Swalen, "Optical and electrical properties of thin silver films grown under ion bombardment," *Phys. Rev. B, Condens. Matter*, vol. 33, no. 2, pp. 879–888, Jan. 1986.

[27] I. Hamberg, C. G. Granqvist, K. F. Berggren, B. E. Sernelius, and L. Engström, "Band-gap widening in heavily Sn-doped In_2O_3," *Phys. Rev. B, Condens. Matter*, vol. 30, no. 6, pp. 3240–3249, 1984.

[28] P. K. Chiu, W. H. Cho, H. P. Chen, C. N. Hsiao, and J. R. Yang, "Study of a sandwich structure of transparent conducting oxide films prepared by electron beam evaporation at room temperature," *Nanosc. Res. Lett.*, vol. 7, no. 1, pp. 1–5, Dec. 2012.

[29] J. Zhou, "Indium tin oxide (ITO) deposition, patterning and Schottky contact fabrication," Rochester Inst. Technol., Rochester, NY, USA, Tech. Rep., 2005.

[30] K. Oura, V. G. Lifshits, A. A. Saranin, A. V. Zotov, and M. Katayama, *Surface Science: An Introduction*, 1st ed. Berlin, Germany: Springer-Verlag, 2010.

[31] J. Hautcoeur, X. Castel, F. Colombel, R. Benzerga, M. Himdi, G. Legeay, and E. Motta-Cruz, "Transparency and electrical properties of meshed metal films," *Thin Solid Films*, vol. 519, no. 11, pp. 3851–3858, Mar. 2011.

[32] A. Martin, X. Castel, M. Himdi, and O. Lafond, "Mesh parameters influence on transparent and active antennas performance at microwaves," *AIP Adv.*, vol. 7, no. 8, pp. 1–8, 2017.

[33] J. Hautcoeur, L. Talbi, K. Hettak, and M. Nedil, "60 GHz optically transparent microstrip antenna made of meshed AuGL material," *IET Microw., Antennas Propag.*, vol. 8, no. 13, pp. 1091–1096, Oct. 2014.

[34] *SMS7630*. Accessed: May 17, 2010. [Online]. Available: https://datasheet.octopart.com/SMS7630-040LF-Skyworks-%0ASolutionsdatasheet-8832283.pdf

[35] N. Eltresy, D. Eisheakh, E. Abdallah, and H. Elhenawy, "RF energy harvesting using efficiency dual band rectifier," in *Proc. Asia–Pacific Microw. Conf. (APMC)*, Nov. 2018, pp. 1453–1455.

[36] R. H. Chen, Y. C. Lee, and J. S. Sun, "Design and experiment of a loop rectenna for RFID wireless power transmission and data communication applications," in *Proc. Prog. Electromagn. Res. Symp.*, 2009, pp. 528–531.

[37] E. F. Da Silva, A. G. Neto, and C. Peixeiro, "Fast and accurate rectenna design method," *IEEE Antennas Wireless Propag. Lett.*, vol. 18, no. 5, pp. 886–890, May 2019.

[38] N. Singh, B. K. Kanaujia, M. T. Beg, N. Mainuddin, T. Khan, and S. Kumar, "A dual polarized multiband rectenna for RF energy harvesting," *AEU Int. J. Electron. Commun.*, vol. 93, pp. 123–131, Sep. 2018.

[39] N. Singh, B. K. Kanaujia, M. T. Beg, N. Mainuddin, S. Kumar, H. C. Choi, and K. W. Kim, "Low profile multiband rectenna for efficient energy harvesting at microwave frequencies," *Int. J. Electron.*, vol. 106, no. 12, pp. 2057–2071, Dec. 2019.

[40] U. Muncuk, K. Alemdar, J. D. Sarode, and K. R. Chowdhury, "Multiband ambient RF energy harvesting circuit design for enabling batteryless sensors and IoT," *IEEE Internet Things J.*, vol. 5, no. 4, pp. 2700–2714, Aug. 2018.

[41] N. A. Eltresy, O. M. Dardeer, A. Al-Habal, E. Elhariri, A. H. Hassan, A. Khattab, D. N. Elsheakh, S. A. Taie, H. Mostafa, H. A. Elsadek, and E. A. Abdallah, "RF energy harvesting IoT system for museum ambience control with deep learning," *Sensors*, vol. 19, no. 20, p. 4465, Oct. 2019.

[42] N. A. Eltresy, O. M. Dardeer, A. Al-Habal, E. Elhariri, A. M. Abotaleb, D. N. Elsheakh, A. Khattab, S. A. Taie, H. Mostafa, H. A. Elsadek, and E. A. Abdallah, "Smart home IoT system by using RF energy harvesting," *J. Sensors*, vol. 2020, pp. 1–14, Dec. 2020.

NERMEEN A. ELTRESY received the B.Sc. and M.Sc. degrees from Menoufia University, Shibin Al Kawm, Egypt, in May 2012 and January 2016, respectively, and the Ph.D. degree in designing and fabrication of RF energy harvesting devices for the IoT applications from Ain Shams University, in 2020. Her master's thesis was about the study of nanoantennas element and arrays for various applications. In addition, the transparent elements and array was a part of the study. She is currently a Researcher with the Microstrip Department, Electronics Research Institute. She has authored or coauthored over 25 papers in periodical journals and international conferences and coauthored one book. Her research interests include transparent antennas, RF energy harvesting, nanoantennas, transmit array, reflect array, and advanced electromagnetic research application using new and complex nanomaterial. She was a recipient of the Best Distinguished Assistant Researcher from the Electronics Research Institute in 2020. She has acted as a Reviewer for the IEEE Internet of Things and IEEE Access Journal.

ABD ELHAMID M. ABD ELHAMID received the B.Sc. degree in physics and the M.Sc. degree in controlling graphene growth by pulsed laser deposition from the National Institute of Laser Enhanced Science, Cairo University. He is currently pursuing the Ph.D. degree in high power miniaturized planner hybrid supercapacitor by nanosecond laser direct writing. As a Research Assistant with the Nanotechnology Laboratory, Electronics Research Institute, he is responsible for associated nanofabrication process and surface science physics. His published papers reported many specialized experiences in thin film deposition techniques, such as PLD, CVD, PECVD, thermal evaporation, and RF/DC sputtering. In May 2020, he had received the Annual Institutional 1st Prize in publishing.

DALIA M. ELSHEAKH (Senior Member, IEEE) received the B.Sc., M.Sc., and Ph.D. degrees from Ain Shams University, in 1998, 2005, and 2010, respectively. Her M.S. Thesis was on the design of microstrip PIFA for mobile handsets and the Ph.D. Thesis was on electromagnetic band-gap structure. She was an Assistant Researcher with the HCAC, College of Engineering, University of Hawai'i, USA, in 2008, and an Assistant Professor, in 2014 and 2018. From 2010 to 2015, she was an Assistant Professor with the Microstrip Department, Electronics Research Institute, where she has been an Associate Professor, since 2016. She has published 55 articles in peer-refereed journals, 50 papers in international conferences, and four books. She holds three patents. She is currently a member of many contracted projects (13 research and development project) as PI funded from many funding agencies, such as ASRT, NTRA, NSF, and STDF.

HADIA M. ELHENNAWY received the B.Sc. and M.Sc. degrees from Ain Shams University, Cairo, Egypt, in 1972 and 1976, respectively, and the Ph.D. degree from the Technische Universität Braunschweig, Germany, in 1982. In 1982, she joined the Electronics and Communications Engineering Department, Ain Shams University, as an Assistant Professor. She was nominated as an Associate Professor, in 1987 and a Professor, in 1992. In 2004, she was appointed as the Vice-Dean for graduate study and research. In 2005, she was appointed as the Dean of the Faculty of Engineering, Ain Shams University. She has been the Head of the Microwave Research Laboratory, since 1982. She has published more than 280 journal and conference papers and supervised more than 50 Ph.D. and M.Sc. students. Her research interests include microwave circuit design, antennas, microwave communication, and recently wireless communication. She is currently a member of the Industrial Communication Committee in the National Telecommunication Regulatory Authority (NTRA), the Educational Engineering Committee in the Ministry of Higher Education, and the Space Technology Committee in the Academy of Scientific Research. She was the Editor-in-Chief of *Scientific Bulletin* from August 2004 to August 2005.

ESMAT A. ABDALLAH (Member, IEEE) graduated from the Faculty of Engineering, Cairo University, Giza, Egypt, in 1968. She received the M.Sc. and Ph.D. degrees from Cairo University, in 1972 and 1975, respectively. She was nominated as an Assistant Professor, an Associate Professor, and a Professor, in 1975, 1980, and 1985, respectively. She supervised more than 80 Ph.D. and M.Sc. theses. She has been the President of the Electronics Research Institute, Egypt, for more than ten years. She has conducted many contracted projects (32 research and development project) as PI funded from many funding agencies, such as ASRT, NTRA, NSF, and STDF. She has six books and seven patents. Her research interests include microwave circuit designs, planar antenna systems, EBG structures, UWB components, and antenna and RFID systems. She has authored and coauthored more than 280 research papers in highly cited international journals and in proceedings of international conferences in her field, such as IEEE Transactions on Antennas and Propagation and IEEE Transactions on Microwave Theory and Techniques.